

The first year of Borexino

D. Franco,* G. Bellini, S. Bonetti, M. Buizza Avanzini, B. Caccianiga, D. D'Angelo, M. Giammarchi, P. Lombardi, L. Ludhova, E. Meroni, L. Miramonti, L. Perasso, and G. Ranucci

Dipartimento di Fisica, Università degli Studi e INFN, 20133 Milano, Italy

J. Benziger

Chemical Engineering Department, Princeton University, Princeton, NJ 08544, USA

L. Cadonati

Physics Department, University of Massachusetts, Amherst, MA 01003, USA

F. Calaprice, A. Chavarria, F. Dalnoki-Veress, C. Galbiati, A. Goretti, Andrea Ianni, M. Leung, B. Loer,

K. McCarty, A. Pocar,[†] and R. Saldanha

Physics Department, Princeton University, Princeton, NJ 08544, USA

C. Carraro, G. Manuzio, M. Pallavicini, S. Perasso, P. Risso, C. Salvo, G. Testera, and S. Zavatarelli

Dipartimento di Fisica, Università e INFN, Genova 16146, Italy

H. de Kerret, D. Kryn, M. Obolensky, and D. Vignaud

Laboratoire AstroParticule et Cosmologie, 75231 Paris cedex 13, France

A. Derbin and V. Muratova

St. Petersburg Nuclear Physics Institute, 188350 Gatchina, Russia

A. Etenko, E. Litvinovich, I. Machulin, A. Sabelnikov, M. Skorokhvatov, and S. Sukhotin

RRC Kurchatov Institute, 123182 Moscow, Russia

K. Fomenko, O. Smirnov, A. Sotnikov, and O. Zaimidoroga

Joint Institute for Nuclear Research, 141980 Dubna, Russia

S. Gazzana, Aldo Ianni, G. Korga, M. Laubenstein, L. Papp, A. Razeto, and R. Tartaglia

INFN Laboratori Nazionali del Gran Sasso, SS 17 bis Km 18+910, 67010 Assergi (AQ), Italy

M. Goeger-Neff, T. Lewke, Q. Meindl, L. Oberauer, F. von Feilitzsch, and M. Wurm

Physik Department, Technische Universität Muenchen, 85747 Garching, Germany

C. Grieb,[‡] S. Hardy, M. Joyce, S. Manecki, R.S. Raghavan, D. Rountree, and R.B. Vogelaar

Physics Department, Virginia Polytechnic Institute and State University, Blacksburg, VA 24061, USA

V. Kobychew

Kiev Institute for Nuclear Research, 06380 Kiev, Ukraine

W. Maneschg, S. Schönert, H. Simgen, and G. Zuzel

Max-Planck-Institut für Kernphysik, 69029 Heidelberg, Germany

F. Masetti, F. Ortica, and A. Romani

Dipartimento di Chimica, Università e INFN, 06123 Perugia, Italy

M. Misiaszek

M. Smoluchowski Institute of Physics, Jagiellonian University, 30059 Krakow, Poland and

INFN Laboratori Nazionali del Gran Sasso, SS 17 bis Km 18+910, 67010 Assergi (AQ), Italy

D. Montanari

INFN Laboratori Nazionali del Gran Sasso, SS 17 bis Km 18+910, 67010 Assergi (AQ), Italy and

Physics Department, Princeton University, Princeton, NJ 08544, USA

Y. Suvorov

Dipartimento di Fisica, Università degli Studi e INFN, 20133 Milano, Italy and

RRC Kurchatov Institute, 123182 Moscow, Russia

M. Wojcik

M. Smoluchowski Institute of Physics, Jagiellonian University, 30059 Krakow, Poland

Borexino is an experiment designed to detect in real-time low energy solar neutrinos. It is installed at the Gran Sasso Underground Laboratory and has started taking data in May 2007. We report the direct measurement of the ${}^7\text{Be}$ solar neutrino signal rate after 1 year of data taking. Implications and perspectives are discussed.

1. Introduction

The Sun is an intense source of electron neutrinos, produced in the nuclear reactions of the proton-proton chain and of the CNO cycle. Solar neutrinos provide a unique probe for studying both the nuclear fusion reactions that power the Sun and the fundamental properties of neutrinos.

*Contribution Presented by D. Franco.

Email: Davide.Franco@mi.infn.it

[†]Now at Stanford University, CA, USA.

[‡]Present address: European Patent Office, Munich, Germany.

In particular, neutrino oscillations, described in the Large Mixing Angle (LMA) Mikheyev-Smirnov-Wolfenstein (MSW) [1, 2] theory, offer a solution to the solar neutrino problem, the long standing discrepancy between the observation of the solar neutrino flux in the pioneer radiochemical and water Cherenkov experiments [3] and the prediction of the Standard Solar Model [4].

A central feature of the LMA-MSW solution is the prediction that neutrino oscillations are dominated by vacuum oscillations at low energies (<2 MeV) and by resonant matter-enhanced oscillations, taking place in the Sun's core, at higher energies (>5 MeV).

Borexino is the first experiment to report a real-time observation of low energy solar neutrinos in the vacuum oscillation regime by the direct measurement of the low energy (0.862 MeV) ${}^7\text{Be}$ solar neutrino interaction rate. We report here the results [5, 6] from an analysis of 192 live days of Borexino detector live-time in the period from May 16, 2007 to April 12, 2008, totaling a 41.3 ton yr fiducial exposure to solar neutrinos.

Solar neutrinos are detected in Borexino through their elastic scattering on electrons in the scintillator. Electron neutrinos (ν_e) interact through charged and neutral currents and in the energy range of interest have a cross section 5 times larger than ν_μ and ν_τ , which interact only via the neutral current. The electrons scattered by neutrinos are detected by means of the scintillation light retaining the information on the energy, while information on the direction of the scattered electrons is lost. The basic signature for the mono-energetic 0.862 MeV ${}^7\text{Be}$ neutrinos is the Compton-like edge of the recoil electrons at 665 keV, as shown in Figure 1.

A strong effort has been devoted to the containment and comprehension of the background, since electron-like events induced by solar neutrino interactions can not be distinguished, on an event-by-event basis, from electrons or photons due to radioactive decays. The main challenge is then to reduce the background in the active mass in order to reach a signal-to-noise ratio equal to 1. The detector has been built following a self shielding design by increasing the radiopurity requirements while moving closer to the active mass. In order to reach a signal-to-noise ratio of 1 an intrinsic radiopurity of $4 \cdot 10^{-4} \mu\text{Bq/kg}$ is required both for ${}^{238}\text{U}$ and ${}^{232}\text{Th}$ contaminations. The Borexino purification strategy relies on filtration at the level of $0.05 \mu\text{m}$, multi-stage distillation and high purity nitrogen sparging.

2. The Detector

The Borexino detector is located at the Gran Sasso National Laboratories (LNGS) in central Italy, at a

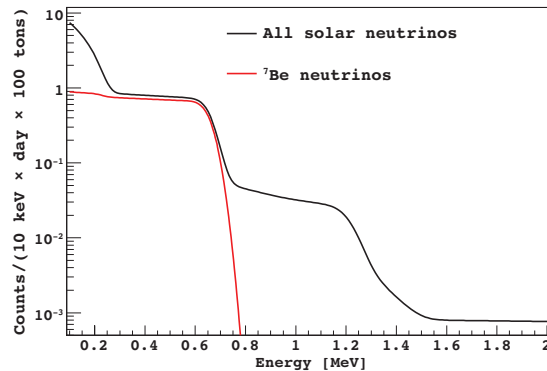


Figure 1: Neutrino spectra expected in Borexino (accounting for the detector's energy resolution). The solid black line represents the neutrino signal rate in Borexino according to the most recent predictions of the Standard Solar Model [4] including neutrino oscillations with the LMA-MSW parameters [2]. The solid red line illustrates the contribution due to ${}^7\text{Be}$ neutrinos. pp neutrinos contribute to the spectrum below 0.3 MeV and the edge at 1.2 MeV is due to p-e-p neutrinos.

depth of 3800 m.w.e.. Neutrinos are detected via elastic scattering off electrons in liquid scintillator. The sketch of the detector is shown in Figure 2. The active target consists of 278 tons of pseudocumene (PC, 1,2,4 trimethylbenzene), doped with 1.5 g/liter of PPO (2,5-diphenyloxazole, a fluorescent dye). The scintillator is contained in a thin ($125 \mu\text{m}$) nylon vessel and is shielded by two concentric PC buffers (323 and 567 tons) doped with 5.0 g/l of a scintillation light quencher (dimethylphthalate). The two PC buffers are separated by a second thin nylon membrane to prevent diffusion of radon towards the scintillator. The scintillator and buffers are contained in a Stainless Steel Sphere (SSS) with a diameter of 13.7 m. The SSS is enclosed in a 18.0-m diameter, 16.9-m high domed Water Tank (WT), containing 2100 tons of ultra-pure water as an additional shield. The scintillation light is detected via 2212 8" photomultiplier tubes (PMTs) uniformly distributed on the inner surface of the SSS. Additional 208 8" PMTs instrument the WT and detect the Cherenkov light radiated by muons in the water shield, serving as a muon veto. A detailed description of the detector can be found in [7].

An *event* in Borexino is recorded when at least 25 PMT pulses occur within a time window of 99 ns (the corresponding energy threshold is about 40 keV). When a trigger occurs, a $16 \mu\text{s}$ gate is opened and time and charge of each PMT pulse is collected. The offline software identifies the shape and the length of each scintillation pulse and reconstructs the position of the energy deposit in the scintillator by means of a time of flight technique. Pulse shape analysis is performed to identify various classes of events, among

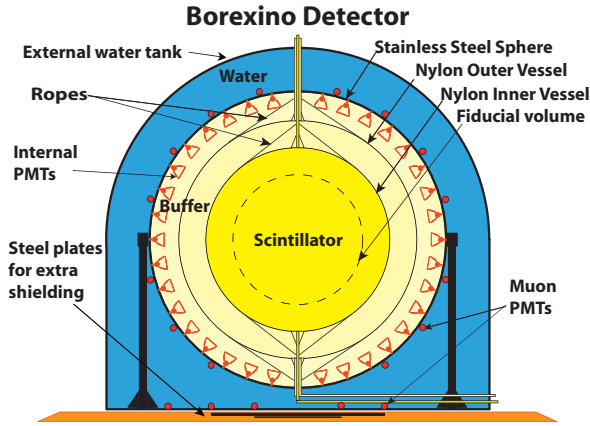


Figure 2: Schematic drawing of the Borexino detector.

which electronic noise, pile up events, muons, α and β particles.

3. Event Selection and Spectral Fits

The analyzed energy range is 250–800 keV. The event selection relies on the following cut criteria:

1. The event must have a unique reconstructed cluster of PMT hits, in order to reject pile-up events and fast coincident events in the same acquisition window. The efficiency of this cut is nearly 100% because the very low triggering rate results in a negligible pile-up.
2. Events with Čerenkov light in the water tank detector are identified as cosmic muons and rejected.
3. All the detector is vetoed for 2 ms after each muon crossing the scintillator. In this way, muon-induced neutrons (mean capture time $\sim 250 \mu\text{s}$) and spurious events like after-pulses are rejected. The measured muon rate in Borexino (muons that cross the scintillator and buffer volume) is $0.055 \pm 0.002 \text{ s}^{-1}$. The dead time introduced by this cut is negligible.
4. Decays due to radon daughters occurring before the ^{214}Bi - ^{214}Po delayed coincidences are vetoed. The fraction surviving the veto is accounted for in the analysis.
5. The events must be reconstructed within a spherical fiducial volume corresponding nominally to 100 ton in order to reject external γ background (Figure 3). Another volumetric cut ($z < 1.8 \text{ m}$) was applied in order to remove a small background from ^{222}Rn daughters

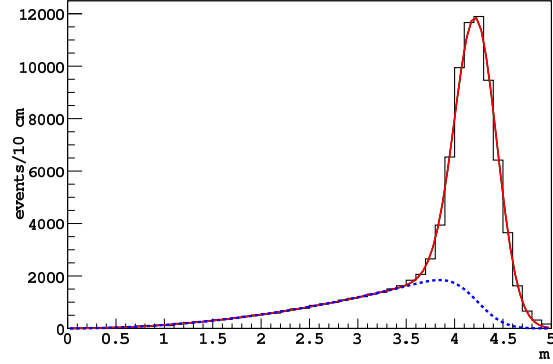


Figure 3: Fit of the radial distribution of the events in the ^7Be energy region. The fit function has two components: bulk events (blue) and events from the nylon vessel and from the buffer (red). The fiducial volume is defined with a radial cut at 3 m.

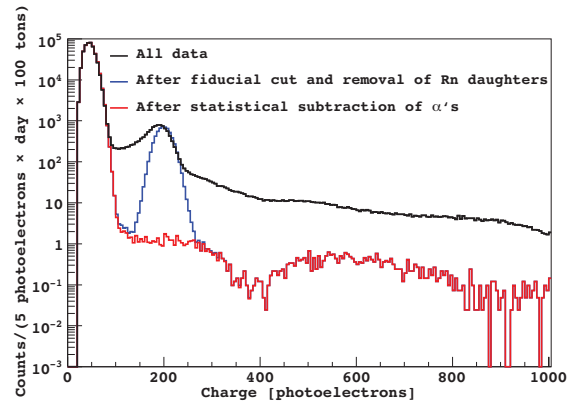


Figure 4: The raw photoelectron charge spectrum after the cuts 1-3 (black), after the fiducial cut 5 (blue), and after the statistical subtraction of the α -emitting contaminants (red). All curves scaled to the exposure of 100 day ton. Cuts are described in the text.

in the north pole of the inner vessel, resulting in a nominal fiducial mass of 87.9 t.

In Figure 4 the measured spectrum in 192 days is shown before and after the cuts. It can be noticed that an important peak is present in the data after the fiducial volume cut. This peak is due to a ^{210}Po contamination still present in the liquid scintillator after purification and filling. ^{210}Po is produced in decay chain segment starting from ^{210}Pb . ^{210}Pb decays to ^{210}Bi which has an end-point energy at about 1 MeV. The measured activity of ^{210}Po is clearly not in equilibrium with a ^{210}Bi source, as shown in Figure 5. Moreover, the measured decay trend has a mean life compatible with ^{210}Po . Even if ^{210}Pb contamination is high with respect to the expected signal, it can be efficiently identified in the offline analysis with the pulse shape discrimination, shown in Figure

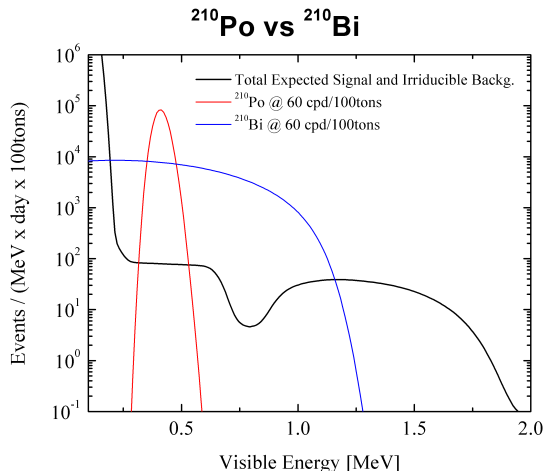


Figure 5: Expected ^{210}Bi contribution in case of ^{210}Pb contamination.

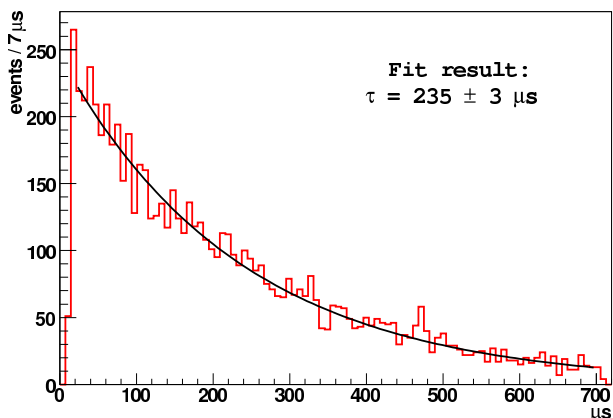


Figure 6: Time difference between the first and second event of the ^{214}Bi - ^{214}Po coincidence sample. The resulting lifetime from the fit ($235 \pm 3 \mu\text{s}$) is in agreement with the ^{214}Po mean life ($237 \mu\text{s}$)

7. A filter based on the time response of the PC-based scintillator [8], slower for α particles than for β 's, discriminates the ^{210}Po events. The red curve in Figure 4 shows the effect of the statistical subtraction of the α -emitting contaminants, by use of the pulse shape discrimination.

The study of fast coincidence decays of ^{214}Bi - ^{214}Po (see Figure 6) and ^{212}Bi - ^{212}Po , yields, under the assumption of secular equilibrium, to the estimation of ^{238}U contamination equal to $(1.6 \pm 0.1)10^{-17}$ g/g and of ^{232}Th equal to $(6.8 \pm 1.5)10^{-18}$ g/g. The ^{85}Kr content in the scintillator was probed by looking the delayed coincidence in the secondary branch of ^{85}Kr decay throughout the metastable level $^{85\text{m}}\text{Rb}$ (BR = 0.43%). Our best estimate for the activity of ^{85}Kr is 29 ± 14 counts/(day·100 ton).

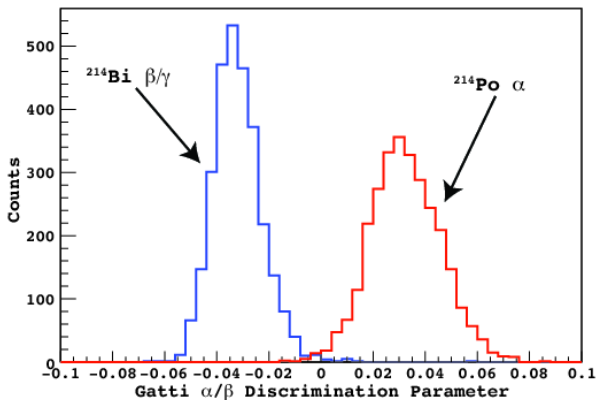


Figure 7: α/β discrimination of ^{214}Bi - ^{214}Po events with the Gatti filter.

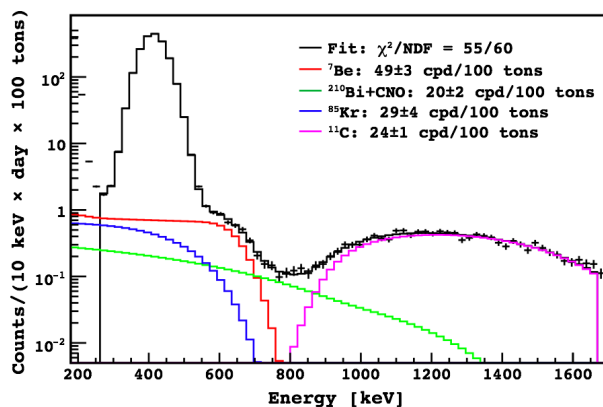


Figure 8: Spectral fit in the energy region 260-1670 keV before the α subtraction.

From the spectrum in Figure 4 the expected Compton-like edge due to ^7Be solar neutrinos is well visible. Moreover, it can be seen that at high energy the spectrum is dominated by a cosmogenic component well known, the ^{11}C . ^{11}C is produced underground by muons interacting with ^{12}C in the liquid scintillator. This background depends on the depth of the underground laboratory [9, 10].

The spectra within the fiducial volume was studied with and without the α statistical subtraction. Results are shown in Figures 8 and 9. In the spectral fits, the contribution of CNO neutrinos is combined with that of ^{210}Bi which is not known. The two spectra are degenerate in the ^7Be region. The ^7Be , the ^{85}Kr , the ^{11}C as well as the light yield are free parameters of the fit. A light yield of about 500 p.e./MeV is found for β 's, and the energy resolution scales approximately as $5\%/\sqrt{E[\text{MeV}]}$

Systematic uncertainties come mainly from the total scintillator mass (0.2%), the fiducial mass definition (6%) and the detector response function (6%).

Taking into account systematic errors, our best value for the interaction rate of the 0.862 MeV ^7Be so-

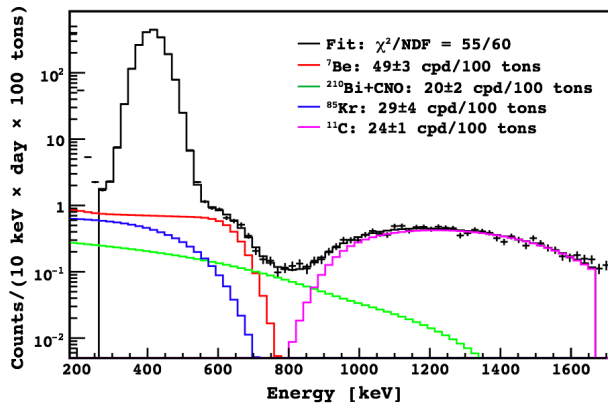


Figure 9: Spectral fit in the energy region 160-2000 keV.

lar neutrinos is 49 ± 3 (stat) ± 4 (syst) counts/(day100 ton). The corresponding flux solar neutrino flux $\Phi(^7\text{Be}) = (5.08 \pm 0.25) \times 10^9 \text{ cm}^{-2} \text{ s}^{-1}$ is evaluated assuming the oscillation parameters, $\sin^2 2\theta_{12} = 0.87$ and $\Delta m_{12}^2 = 7.6 \times 10^{-5} \text{ eV}^2$, from [2], in good agreement with expectations.

4. Results and Perspectives

The expected neutrino interaction rate in case of no oscillations is 74 ± 4 counts/(day100 ton). The Borexino measurement of the ^7Be neutrino rate confirms the oscillation hypothesis at 4σ , in agreement with the MSW-LAM prediction.

Under the assumption of the SSM constraint the solar neutrino survival probability is measured to be $P_{ee} = 0.56 \pm 0.10$.

The Borexino measured rate can be combined with the other solar neutrino measurements to constrain the flux normalization constants of the other solar neutrino fluxes. This leads to the best determination of the pp solar neutrinos flux, obtained with the assumption of the luminosity constraint: $f_{pp} = 1.005_{-0.020}^{+0.008}$ where f_{pp} is the ratio between the measured and predicted pp neutrino fluxes. With the same technique, Borexino obtained the best limit on the CNO flux: $f_{CNO} < 6.27$ (90% C.L.).

The low energy solar neutrino spectrum is sensitive to the possible presence of a non-null magnetic moment. We exploited this feature to determine the best upper limit to the neutrino magnetic moment ($5.4 \times 10^{-11} \mu\text{B}$, 90% C.L.) [6].

The first Borexino results have shown for the first time the feasibility to measure solar neutrinos in the sub-MeV range in real-time. Moreover, the high level of radiopurity achieved allows to investigate other so-

lar neutrino sources. In particular, CNO and p-e-p neutrino detections depend on the possibility to tag and reject event by event cosmogenic ^{11}C background. This goal is at present under investigation, since ^{11}C can be identified by means of the three-fold coincidence with the parent muon and the following neutron emission and capture on hydrogen.

Thanks to the excellent scintillator radio-purity, Borexino has also the opportunity to measure the ^8B neutrino spectrum with the lowest energy threshold so far. A dedicated analysis with the energy threshold at 2.8 MeV is in progress.

References

- [1] S.P. Mikheev and A.Yu. Smirnov, Sov. J. Nucl. Phys. **42**, 913 (1985); L. Wolfenstein, Phys. Rev. D **17**, 2369 (1978); P.C. de Holanda and A.Yu. Smirnov, JCAP 0302, 001 (2003).
- [2] S. Abe et al., (KamLAND Collaboration), arXiv:0801.4589v2, submitted to Phys. Rev. Lett. (2008).
- [3] B.T. Cleveland et al., Ap. J. **496**, 505 (1998); K. Lande and P. Wildenhain, Nucl. Phys. B (Proc. Suppl.) **118**, 49 (2003); R. Davis, Nobel Prize Lecture (2002). W. Hampel et al. (GALLEX Collaboration), Phys. Lett. B **447**, 127 (1999); J.N. Abdurashitov et al. (SAGE collaboration), Phys. Rev. Lett. **83**, 4686 (1999); M. Altmann et al. (GNO Collaboration), Phys. Lett. B **616**, 174 (2005); K.S. Hirata et al. (KamiokaNDE Collaboration), Phys. Rev. Lett. **63**, 16 (1989).
- [4] J.N. Bahcall, A.M. Serenelli, and S. Basu, Astrophys. J. Suppl. **165**, 400 (2006); C. Peña-Garay, talk at the conference "Neutrino Telescopes 2007", March 6-9, 2007, Venice, <http://neutrino.pd.infn.it/conference2007/>; A. Serenelli, private communication.
- [5] C. Arpesella et al. (Borexino Collaboration), Phys. Lett. B **658**, 101 (2007).
- [6] C. Arpesella et al. (Borexino Collaboration), accepted for publication on Phys. Rev. Lett., arXiv:0805.3843 (2008).
- [7] G. Alimonti et al. (Borexino Collaboration), submitted to Nucl. Instr. Meth. A, arXiv:0806.2400 (2008).
- [8] H.O. Back et al. (Borexino Collaboration), Nucl. Instrum. Meth. A **584** 98-113 (2008);
- [9] C. Galbiati et al., Phys.Rev.C **71** 055805 (2005).
- [10] H. Back et al. (Borexino Collaboration), Phys. Rev. C **74**, 045805 (2006).